

A nonlinear static approach for curve editing

Rhaleb Zayer

▶ **To cite this version:**

Rhaleb Zayer. A nonlinear static approach for curve editing. Computers and Graphics, 2012, 36 (5), pp.514-520. 10.1016/j.cag.2012.03.024 . hal-00763434

HAL Id: hal-00763434
https://inria.hal.science/hal-00763434

Submitted on 10 Dec 2012

HAL is a multi-disciplinary open access archive for the deposit and dissemination of scientific research documents, whether they are published or not. The documents may come from teaching and research institutions in France or abroad, or from public or private research centers.

L'archive ouverte pluridisciplinaire **HAL**, est destinée au dépôt et à la diffusion de documents scientifiques de niveau recherche, publiés ou non, émanant des établissements d'enseignement et de recherche français ou étrangers, des laboratoires publics ou privés.

A nonlinear static approach for curve editing

Rhaleb Zayer

Inria Nancy Grand-Est and LORIA

Abstract

This paper introduces a method for interactively editing planar curves subject to positional and rotational constraints. We regard editing as a static deformation problem but our treatment differs from standard finite element methods in the sense that the interpolation is based on deformation modes rather than the classic shape functions. A careful choice of these modes allows capturing the deformation behavior of the individual curve segments, and devising the underlying mathematical model from simple and tractable physical considerations. In order to correctly handle arbitrary user input (e.g. dragging vertices in a fast and excessive manner), our approach operates in the nonlinear regime. The arising geometric nonlinearities are addressed effectively through the modal representation without requiring complicated fitting strategies. In this way, we circumvent commonly encountered locking and stability issues while conveying a natural sense of flexibility of the shape at hand. Experiments on various editing scenarios including closed and non-smooth curves demonstrate the robustness of the proposed approach.

1. Introduction

1.1. General problem

Curves are one of the most studied primitives in computer graphics. Over the last decades, concepts from numerical approximation, differential geometry, computational geometry, and mechanics, have contributed to deepen understanding of curves and widen their range of applications. A desirable property when modeling/editing curves is the ability to emulate the deformation behavior of natural objects (e.g. wood, cables),see figure1. Such physical considerations have been present in curve modeling since the early days. They are behind several well established tools e.g. spline curves [1]. In animation, several models for curve-like object simulation have been proposed in the last few years spanning the dynamics of hair, threads, ropes and cables.

In this paper, we regard a curve as a set of connected segments and we are concerned with finding its static equilibrium i.e. positions of the segments' end points when subjected to loading or rotation moments. We identify the following properties as requirements for a satisfactory editing experience;

- robustness to arbitrary user input
- robustness to curve nature (smooth/nonsmooth, open/closed)
- handling of rotation and displacement constraints
- control over global and local effect of deformation
- no wiggling or oscillation during the interaction
- similarity to the deformation of familiar objects e.g threads

Some of these requirements are fulfilled to varying extents in existing works but we are not aware of a method which guarantees full satisfaction of all of them.

Although there has been substantial work on curve deformation in the spatial setting, the planar counterpart did not receive as much attention. With a few exceptions, e.g. [2, 3], there are not many specialized variants for the planar setting. Essential differences between both settings make tailoring the mathematical deformation model from the ground up in the planar configuration more attractive than restricting a spatial formulation to the plane. Planar rotations are fundamentally different from spatial rotations as they are commutative and can be parameterized by a single degree of freedom. This has even a deeper impact on equilibrium relations as planar moments are conservative whereas spatial moments are not necessarily so (different rotation paths would not necessarily lead to the same final configuration). Therefore, developing a planar formulation allows taking advantage of these fundamental properties and simplifies the numerical treatment to a great extents. In the spatial setting, intermediate formulations,

e.g. quaternions, are needed for carrying out algebraic operations and the interpretation of moments gets more intricate. Such problems are still an active research area in both engineering and mathematics [4].

1.2. Contribution

Our approach relies on the concept of natural deformation modes. The general theory is outlined in the context of computational mechanics in [5]. We apply this concept to planar curve editing and derive the full underlying mathematical model. By considering deformation modes which span the degrees of freedom of a curve segment (beam), we can relate displacements to forces by mere visual inspection as illustrated later in equation (1) and related figures (4, 5). This simplicity is made possible by the assumption that local deformations of the curve segments remain small. To a certain extent, our approach bears some similarity to the work of [6] where a modular approach to deformation is taken. Each deformation module is composed of a rest shape, a gross deformation and fine wave deformation. The main difference is that our construction is done at a finer level (individual curve segment). This allows covering all possible deformation modes (of a segment) and maintaining a close check on the physics. In this way, the general formulation is independent of the adopted bending theory and can easily accommodate the standard Euler-Bernoulli theory or the more complex Timoshenko beam theory, see, e.g.,[7] for a description of these theories.

When an object undergoes a large deformation, the assumption that external forces take effect on the initial undeformed geometry is no longer valid. This assumption is implicitly made in the linear deformation setting discussed above. If used for large deformation, the solution drifts away (e.g excessive shape dilation as in figures (6,7)-top). In practice, forces need not be large to lead to a nonlinear behavior. Take for instance the buckling of a straw under compressive forces at its ends. In this case, even minimal forces would have a large impact on the geometry. It is therefore necessary to address geometrically nonlinear aspects of deformation correctly and efficiently (sec.3.4) in order to allow a satisfactory user interaction. We achieve this goal using an iterative scheme where the symmetric tangent stiffness is fully updated at each iteration. Special attention is given to step control in order to drive convergence.

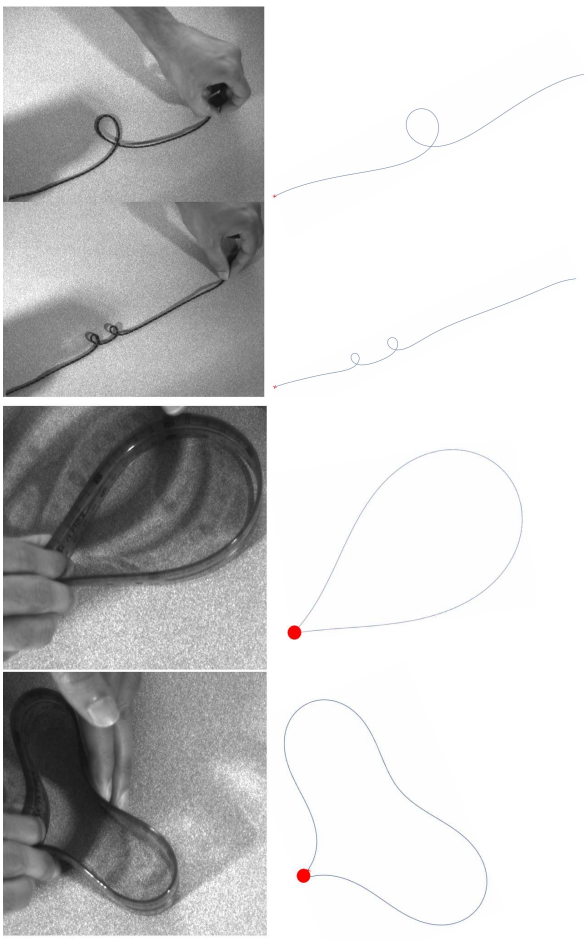


Figure 1: Real deformation of a thread line (right) and a "twist'n flex" ruler compared to the static editing of an initially straight curve.

2. Related work

Many of the existing rod deformation approaches are based on Elastica theory. This theory dates back to work of Euler on the deflection of structures. A generalized treatment has been outlined in the work of the Cosserat brothers [8]. In this formulation, a curve is regarded as a uni-dimensional oriented medium composed of curve segments. The cross-section of each segment endpoints is oriented by a local frame (two covariant vectors and a director). A modern treatment of the theory can be found in [9] which further explored applications of the theory to DNA looping. In computer graphics, the strands model was introduced in [10] for modeling the statics of a surgical wire. An enhanced spring-mass model which takes advantage of quaternion representation was proposed in [11] and demonstrated for cable rooting. The work of [12] proposed an extensive treatment of contact dynamics. Simulation of phenomena such as knotting and dynamic looping (plectoneme formation) was investigated in [13] where parallel transport theory is used to carry out force computa-

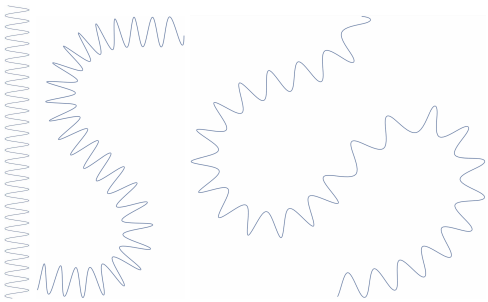


Figure 2: Editing of a sinusoidal curve (left) using moderate deformation (middle) and slightly larger deformation (right). The underlying initial shape of the curve is preserved.

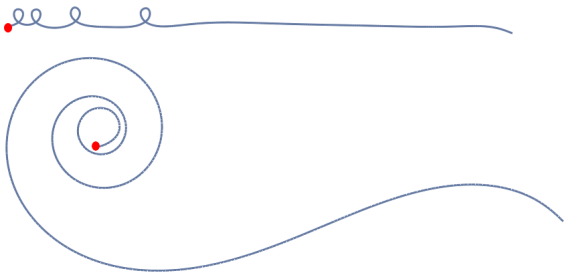


Figure 3: Illustration of the robustness of our approach to multiple loopings (top) and large rotations (bottom) where the user drags the free end in circular manner.

tion. All the above mentioned approaches operate in the spatial setting and specialized variants for the planar setting have been studied less. A notable exception is the planar variant of super-helices [14]. Super-helices offer several improvements over the original strands model particularly in runtime. The planar version features super-circles as a primitive for curve animation in [3].

In the latter approach however, the editing is limited to smooth curves (where a geometric fitting is possible) and neither closed contours nor sharp corners can be handled. Furthermore it is required that the curve be clamped at one end. The goal of the current work is to present an approach that does not requires any specialized fitting primitives and can address the issues related to the nature of the curve (smooth/nonsmooth) and multiple constraints.

In mesh editing, more methods favor a static approach to deformation, see e.g. the survey work [15]. Some of these methods can be adapted to curve deformation as demonstrated in [2]. This two-step approach does not explicitly address the nonlinear aspects of deformation and this leads to some undesirable effects such as the severe shrinkage illustrated in figure (10-top) (results generated using online demo [16] kindly made available by the authors). Our approach addresses such limitations efficiently as illustrated in figure (10-bottom).

In the structural engineering community, key theoretical ideas for modeling beam deformation can be found in [17] and [18]. Finite elements models based on these representations requires additional care to deal with shear locking and may yield non-symmetric tangent stiffness matrices during the iterative Newton based solution, see e.g. [4]. This issue may have deep impact on performance, "in certain cases where the exact tangent stiffness matrix is not symmetric, the extra iterations required by a symmetric approximation to the tangent matrix use less computer time than solving the nonsymmetric tangent matrix at each iteration" [19].

An alternative treatment is the so called co-rotational approach (see [20] for a general introduction) which addresses deformations involving large rotations and small proper body deformation (strain). Simplified variants of this theory have been introduced for volumetric deformation in computer graphics, see e.g. [21, 22]. In the simplified co-rotational setting, considerable speedup has been achieved for solid elements as the stiffness is not recomputed but simply warped throughout the deformation. Further improvements with regards to stability and robustness have been presented in subsequent work, e.g. [23]. Adopting the stiffness-warping idea alone to our problem would not fully account for geometric nonlinearities (e.g. buckling which is commonly encountered in slender objects) and can lead to undesirable effects especially when deformations are too large. Such effects are illustrated in figures (6-top), and (7-left). In both examples the linear stiffness is co-rotated and updated within an iterative Newton scheme.

Our work operates also in convected coordinates but more emphasis is put on geometric nonlinearities and their contribution towards the tangent stiffness which drives the iterative Newton scheme towards static equilibrium.

3. Planar deformation

As mentioned in the introduction, we take advantage of the natural mode approach [5]. We are not aware of any use of this concept to the planar curve setting, therefore we propose a full derivation of the numerical model. The key idea is to define a set of intuitive (natural) deformation modes.

The deformation of the individual segments of a curve can be decomposed into a set rigid body motions

which capture the evolution of the local frame attached to the element with respect to a fixed coordinate system, and a set of deformation shapes within the local frame (Section 3.1). This separation offers many advantages. First, the deformation within the local frame is small in general and can be approximated using linear elasticity (Sections 3.2 and 3.3). Second, the simplicity of our model allows for capturing geometric nonlinearities through simple but practical approximation (Section 3.4).

Although there is a similarity to standard finite elements in the sense that we aim at establishing a relation between loading and displacement, the current derivation deviates from standard finite elements as we do not rely on shape functions but rather on deformation modes. This yields concise representations see e.g equation (5). Shape functions often reduce the problem to numerical fitting, this often hides the physical nature of the problem. Deformation modes on the other hand bring forward this physical aspect into the heart of the numerical modeling.

As we restrict ourselves to the planar setting, we capitalize on the vector nature of planar rotations which ceases to hold in higher dimensions.

3.1. Deformation modes

In the following bold font will be used to denote vectors and matrices. Scalars will use normal fonts.

Consider an initially straight segment of length ℓ in the xy-plane. Let E be its elastic modulus, G its shear modulus, A its cross-sectional area and I the inertia. In all our experiments these parameters were resp. set to 1,1,3 and 1. The segment is completely defined by the location of its endpoints. On each of the two nodes act three forces, and these are (in a Cartesian frame attached to midpoint of the segment) a force F_x in the x-direction, a force F_y in the y-direction and a bending moment M that leads to a rotation around the z-axis (perpendicular to the plane). The element displacements arising therefrom are, accordingly, the displacements u_x, u_y, and a rotation u_θ.

We are concerned with establishing a relationship between the displacements of the nodes $\mathbf{u}$ and the force $\mathbf{f}$ acting on them. $\mathbf{u} = (\mathbf{u}_1, \mathbf{u}_2)^T$, $\mathbf{u}_i = (u_{ix}, u_{iy}, \theta_i)^T$ where i=1,2. The corresponding element forces that work conjugately to these displacement are $\mathbf{f} = (\mathbf{f}_1, \mathbf{f}_2)^T$, $\mathbf{f}_i = (F_i x, F_i y, M_i)^T$.

In order to establish such a relation it is worthwhile to consider a set of forces and displacements that spans the range of the six degrees of freedom. The selection of these forces and displacements could be arbitrarily, it only has to represent linearly independent deformations. Conveniently, the deflection of an element can be decomposed into a set of rigid form of movements $\mathbf{r}_O$ which correspond to rigid body motions and set of proper body deformation (stretching and bending) $\mathbf{r}_N$.

Rigid body modes may be chosen as the translations r_{O1} along the x-axis, r_{O2} along the y-axis, and the rotation r_{O3} around the z-axis, see figure 4. These modes are clearly independent and span the range of all possible rigid body motions.

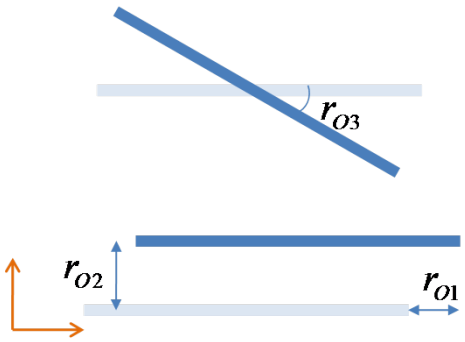


Figure 4: Rigid body displacement of a planar beam

There remain three additional deformation modes to be assigned. These may be chosen so as to capture the deformation of the beam in its local frame. Extension along the central axis is uniquely defined and can be then selected as the first deformation mode. The remaining bending modes may be defined as symmetric bending and anti-symmetric bending as illustrated in figure (5). These natural deformation modes seem to be the most convenient choice as bending is captured using only two modes in contrast to standard finite element representations, where generally four shape function are needed [7].

The natural displacements depicted in figures (4) and (5) can be related to the cartesian displacement in the local frame through a transformation matrix which is obtained by visual inspection.

$$\begin{pmatrix} u_{1x} \\ u_{1y} \\ u_{1\theta} \\ u_{2x} \\ u_{2y} \\ u_{2\theta} \end{pmatrix} = \begin{pmatrix} 1 & 0 & 0 & -1/2 & 0 & 0 \\ 0 & 1 & -\ell/2 & 0 & 0 & 0 \\ 0 & 0 & 1 & 0 & 1/2 & 1/2 \\ 1 & 0 & 0 & 1/2 & 0 & 0 \\ 0 & 1 & \ell/2 & 0 & 0 & 0 \\ 0 & 0 & 1 & 0 & -1/2 & 1/2 \end{pmatrix} \begin{pmatrix} r_{O1} \\ r_{O2} \\ r_{O3} \\ r_{N1} \\ r_{N2} \\ r_{N3} \end{pmatrix} \quad (1)$$

Rigid motions do not induce any stress in the curve segment. As such, their conjugate forces and moments do not contribute towards equilibrium. By inverting the

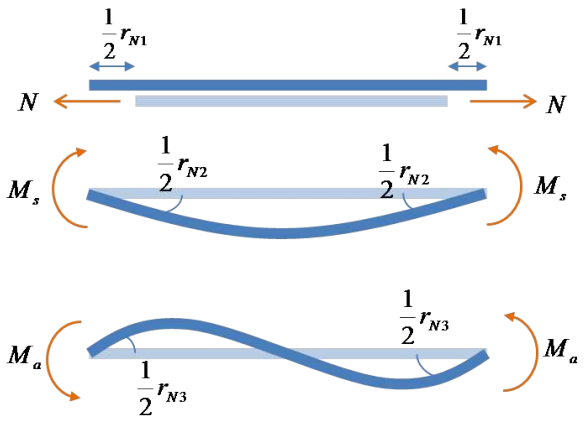


Figure 5: Natural modes of the beam element. The extension forces N, the symmetric bending moments M_s act in opposite directions, and the anti-symmetric moments M_a.

matrix of equation 1 and restricting the relation only to the natural deformation modes can write

$$\mathbf{r}_N = \begin{pmatrix} -1 & 0 & 0 & 1 & 0 & 0 \\ 0 & 0 & -1 & 0 & 0 & 1 \\ 0 & 2/\ell & 1 & 0 & -2/\ell & 1 \end{pmatrix} \mathbf{u} = \mathbf{A}\,\mathbf{u} \tag{2}$$

By means of the contragredient principle, forces which are conjugate to the natural displacement $\mathbf{r}_N$ and cartesian displacements $\mathbf{u}$ can be related by:

$$\mathbf{f} = \mathbf{A}^T\,(N,\ M_s,\ M_a)^T = \mathbf{A}^T\mathbf{f}_N. \tag{3}$$

3.2. Virtual work

According to the principle of virtual work, a system is in equilibrium if the internal work is equal to the external work for all choices of the virtual displacement field [24]. For our case, this reads:

$$\begin{aligned} &\delta\mathbf{f}_1^T\,\mathbf{u}_1 + \delta\mathbf{f}_2^T\,\mathbf{u}_2 + \int_0^l \delta\mathbf{f}^T\,\mathbf{u}\,dx = \\ &\int_0^l \left(\frac{\delta F_x\,F_x}{E\,A} + \frac{\delta F_y\,F_y}{G\,A} + \frac{\delta M\,M}{E\,I}\right)dx; \end{aligned} \tag{4}$$

where the load increment $\delta\mathbf{f} = (\delta f_x,\ \delta f_y,\ \delta m)$ represents the per-unit-length external virtual loads, and δF_x, δF_y, δM refer to the virtual internal forces.

By plugging the forces and displacements depicted in figure 5 into the virtual work equations, see appendix Appendix A, we can arrange the resulting equations in matrix form as

$$\begin{pmatrix} N \\ M_s \\ M_a \end{pmatrix} = \begin{pmatrix} \frac{E\,A}{\ell} & 0 & 0 \\ 0 & \frac{E\,I}{\ell} & 0 \\ 0 & 0 & \frac{3\,E\,I}{(1+\Psi)\ell} \end{pmatrix} \begin{pmatrix} r_{N1} \\ r_{N2} \\ r_{N3} \end{pmatrix} \tag{5}$$

This establishes the relation between the deformation modes and their corresponding displacements, and could be written compactly as $\mathbf{f}_N = \mathbf{K}_N\mathbf{r}_n$, through the natural stiffness $\mathbf{K}_N$.

To obtain the stiffness in the convected cartesian coordinates we use equation 3 to carry out the coordinate transformation

$$\mathbf{f} = \mathbf{A}\,\mathbf{K}_N\,\mathbf{A}^T\,\mathbf{u} = \mathbf{K}\,\mathbf{u} \tag{6}$$

3.3. Equilibrium relations

The derivation above was established in the local frame convecting with the individual curve segments. Now, turn to equilibrium relations in the global frame. let $\mathbf{u}_g = (\mathbf{u}_{g1}, \mathbf{u}_{g2})^T$ be the beam displacement in the global fixed frame. The global forces acting on the nodes are as $\mathbf{f}_g = (\mathbf{f}_{g1}, \mathbf{f}_{g2})^T$.

In the plane, the global frame and the convected frame can be related by a rotation matrix $\mathbf{R}_\theta$

$$\mathbf{R}_\theta = \begin{pmatrix} \cos\theta & -\sin\theta & 0 \\ \sin\theta & \cos\theta & 0 \\ 0 & 0 & 1 \end{pmatrix}; \tag{7}$$

where θ is the angle between the curve segment and the horizontal line (global x-axis). For convenience let's denote by $\mathbf{R}$ the rotation matrix that acts on the beam as a whole

$$\mathbf{R} = \begin{pmatrix} \mathbf{R}_\theta & \\ & \mathbf{R}_\theta \end{pmatrix} \tag{8}$$

in this way $\mathbf{u}_g = \mathbf{R}\,\mathbf{u}$.

In order to obtain the tangent stiffness, we can look at the generalized force,

$$\mathbf{f}_g = \mathbf{R}\,\mathbf{f} = \mathbf{R}\,\mathbf{A}\,\mathbf{f}_N; \tag{9}$$

by reasoning on the incremental force $d\mathbf{f}_g$, we have

$$d\mathbf{f}_g = \underbrace{\mathbf{R}\,\mathbf{A}\,d\mathbf{f}_N} + \underbrace{\mathbf{R}\,d\mathbf{A}\,\mathbf{f}_N + d\mathbf{R}\,\mathbf{A}\,\mathbf{f}_N} \tag{10}$$

By virtue of equations 2 and 3, the first term on the right hand side can be written as $\mathbf{A}\,\mathbf{K}_N\,\mathbf{A}^T\,\mathbf{u}$. The remaining two terms can be expanded explicitly and then rearranged in matrix form as $\mathbf{K}_c\,\mathbf{u}$, this can be done by hand or using symbolic software. $\mathbf{K}_c$ accounts for the variation of the transformation matrices $\mathbf{R}$ and $\mathbf{A}$. This yields

$$d\mathbf{f}_g = \mathbf{R}(\mathbf{A}\,\mathbf{K}_N\,\mathbf{A}^T + \mathbf{K}_c)d\mathbf{u}. \tag{11}$$

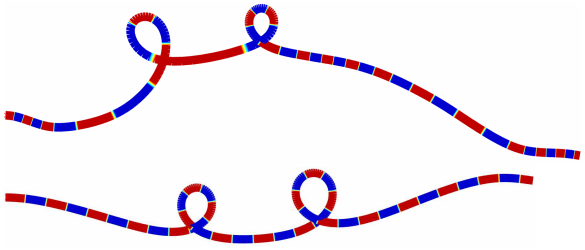


Figure 6: Editing of a straight curve (making two knots and pulling to the right). Leaving out the nonlinearity correction causes the individual curve segments to elongate unnecessarily (top). Including it yields a more consistent deformation geometry (bottom). In both cases the same Newton solver was used.

Keeping in mind that the displacement in the local frame $\mathbf{d}u$ transforms to global coordinates via $\mathbf{R}^T$, the last equation could be written as

$$d\mathbf{f}_g = \mathbf{R}\,\mathbf{K}\,\mathbf{R}^T\,d\mathbf{u}_g = \mathbf{K}_g\,d\mathbf{u}_g; \tag{12}$$

This completes the description of the element stiffness matrix.

3.4. Nonlinearity correction

So far, we did not explicitly address the nonlinear aspects of the deformation. These can be incorporated by means of the elongation of the beam induced by the symmetric and anti-symmetric bending modes. Taking an arclength parametrization of the corresponding quadratic and cubic parabolas (see figure 5), $\zeta = \frac{2}{\ell}x$, ζ in $[-1, 1]$

$$du_y = (1 - \zeta^2)\,\ell/8\,r_{N2} \tag{13}$$

$$du_y = \zeta\,(\zeta^2 - 1)\,\ell/8\,r_{N3} \tag{14}$$

and plugging each separately into the internal virtual work increment (derived from equation (4))

$$\int_0^l (\delta u_y''\,E\,I du_y'' + \delta u_y'\,N\,du_y')dx; \tag{15}$$

reveals the nonlinear relation between the deformation modes and their displacement counterparts.

$$\mathbf{K}_{nonlinear} = 2\,N\,\ell \begin{pmatrix} 0 & 0 & 0 \\ 0 & 1/24 & 0 \\ 0 & 0 & 1/40 \end{pmatrix} \tag{16}$$

This matrix may be added to K_N to account for nonlinear effects of the deformations. Note that the nonlinearity is addressed in the local frame.

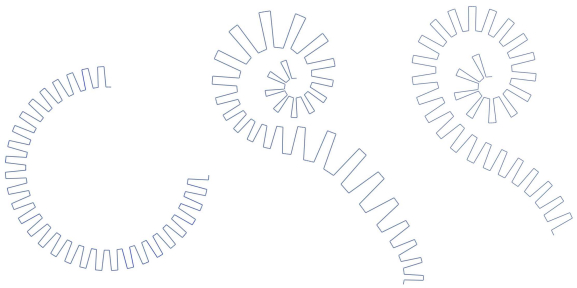


Figure 7: Impact of the nonlinear term on the deformation of a nonsmooth curve (left). Without nonlinearity correction, features get distorted in an unpredictable way and the shape gets elongated (middle). On the other hand the nonlinearity correction (eq.16) preserves feature shapes and size (right). In both cases the same Newton solver was used.

4. Numerical procedures and constraints

To solve the current nonlinear deformation problem, iterative algorithms are unavoidable. The stiffness matrix (equation (12)) and the force vector (equation (10)) can be used within a standard Newton-Raphson approach to carry out the numerical solution. In our experiments this approach works well, but a slightly better performance can be achieved when enhanced with a path following approach [25]. Our experiments with different speedup strategies such as the modified Newton-Raphson or BFGS suggest that if the deformations are moderate, good convergence rates can be achieved. However when the user imposes excessively large deformations the nonlinearities involved cannot be addressed by these approximative techniques and accurate second order computations are required. This motivates the need for the additional nonlinear term in equation (16).

Positional constraints are enforced using Lagrange multipliers to guarantee full satisfaction of user requirements and maintain the symmetry of the system stiffness matrix. Pinned vertices can be completely inactive when all their degrees of freedom are disabled. Alternatively they could be allowed to slide along the x-axis, y-axis or allow rotations to pass through (see the accompanying video).

Although we operate in the nonlinear regime, interactive rates are maintained for most of practical problems. The reasons being: the topological nature of curves is rather simple and yields highly sparse system matrices in which the non zeros line up pretty much along the diagonal. Furthermore, in our formulation, the tangent stiffness is symmetric by construction, a property which makes them solver friendly. In classical finite elements approaches formulated in global coordinates this is not

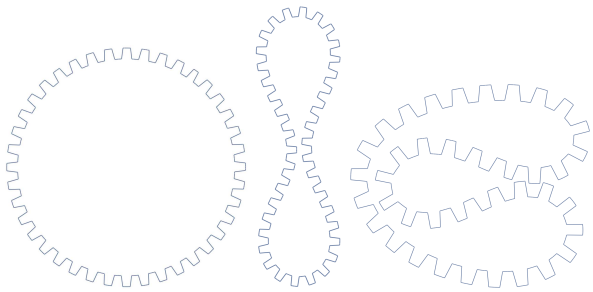


Figure 8: Editing of a closed nonsmooth shape. The approach maintains the original features

generally the case, see e.g. [26] for an overview and discussion on this matter. This property cannot be emphasized enough as it deeply affect the convergence rate which is crucial in an interactive system.

5. Results

We applied our technique to various editing situations. Figure 1 compares our approach to the deformation of real slender objects. Even though the deformations are large the techniques manages to reproduce the natural behavior observed in the real setup.

Our approach can handle curves made of few thousands of vertices while maintaining interactive rates. In general, such lines are smooth enough for practical use. If necessary, several strategies can be adopted to make the edited curve a few folds denser and smoother. The simplest is by generating a spline curve using uniform subdivision. The idea is to attach a subdivision curve S_0 to the coarse initial curve. The coarse curve being used for carrying out the deformation calculations. After each calculation the deformed coarse curve is subdivided following the same scheme as for S_0. In this way, a one to one correspondence to the initial subdivision curve is maintained.

Figure 2 shows an example of a smooth open sinusoidal curve being edited using our approach. Figure 8 illustrates the case of a closed nonsmooth curve. In both settings, the features are preserved. Our approach can preserve shape details as long as the user does not deliberately alter it e.g. by pulling close vertices far apart.

Figure 3 demonstrates the robustness of our approach to extremely the large rotations. In this scenario, a helicoidal shape and multiple loops are obtained by combining rotational and displacement constraints.

Figure 9 shows an example of editing a slender image. The image is deformed as a texture attached to a grid mesh around the curve. When the curve deforms, the mesh position is updated and the texture follows. The material properties described at the beginning of section 3.1 may be adapted to the nature of object at hand to enhance the user's feel of its rigidity or flexibility.



Figure 9: Typical editing results of our approach. Original paisley texture image (bottom) and the results of deforming the centreline curve of the image (top). Top images are slightly scaled for visibility.

The accompanying video shows different editing scenarios using our method. The user can impose constraints on any of the available degrees of freedom. Curve manipulation is achieved by dragging free vertices or imposing a moment to induce a rotation. The editing sessions demonstrate the robustness and ease of use of our technique. A comparison to the method of [3] is also provided using demo code gracefully made available by the authors of the original work. In the latter approach the editing is limited to pinning one end of a smooth curve and dragging the free end. In our experiments the curve tends to snap back when the deformation gets large.

Figure 10 opposes our approach to the one of [2]. We tried to reproduce the initial sketched curve shown in black using an arc segment which we edited using our method. The figure shows that we overcome the severe shrinking suffered by their approach.

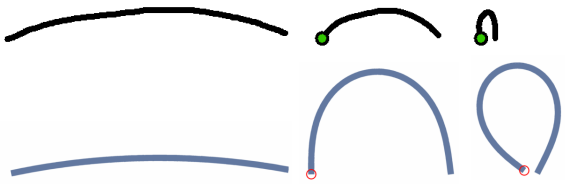


Figure 10: The method of [2] (top) compared to our approach (bottom). The rest shape (left) is edited by fixing the marked vertex and dragging the free end parallel to the horizontal line. Note that our approach does not suffer from the severe shrinkage noticeable on top.

6. Conclusion

A method for editing curves and slender objects in a physically consistent manner was presented. Typi-

cal editing examples are substantiated in the text and the accompanying media. The current implementation is restricted to finding the static equilibrium of curves and addresses issues related to large deformation effects. Nonlinear material behavior is not addressed in the current implementation but could be an interesting venue for future research. Further interesting issues relating to contact, friction, and space curves will be also considered in future work.

Acknowledgments and Credits: The author would like thank Laurent Alonso, Bruno Lévy, Nicolas Ray, Dmitry Sokolov and the anonymous reviewers for their feedback on the paper. This work was funded by the ANR (Agence Nationale de la Recherche) under grant (PhysiGrafix ANR-09-CEXC-014-01).

Appendix A. Local mode relations

For the elongation force depicted in figure 5, we have $F_{1x} = -N$, $u_{1x} = -du/2$, $F_{2x=N}$ and $u_{2x} = du/2$, all the remaining terms correspond to zeros. Substitution into the virtual work equation (4) yields, $r_{N1} = \frac{\ell}{E\,A}N$; Similarly, for the symmetric bending mode we have $r_{N2} = \frac{1}{2}\frac{\ell}{E\,A}M_s$.

For the anti-symmetric bending, the moment is not constant throughout the segment length and it can be interpolated as $M(x) = M_a\,(2x - \ell)/\ell$. By virtue of equation 3 an additional shear force appears $F_{1y} = M_a/\ell$ and $F_{2y} = -Ma/\ell$ when the bending moments are applied. Plugging the bending moments and shear forces into the virtual work equation reveals the relation between the moment and the deformation angle $r_{N3} = \frac{1}{2}\frac{\ell}{E\,I}(1+\Psi)M_s$ where $\Psi = 12\frac{E\,I}{G\,A\,\ell^2}$; this derivation falls within the Timoshenko beam theory as it account for shear deformation. Setting $\Psi = 0$ brings us into the Euler-Bernoulli theory.

References

[1] R. Levien, From spiral to spline: Optimal techniques in interactive curve design, Ph.D. thesis, University of California, Berkeley (2009).

[2] T. Igarashi, T. Moscovich, J. F. Hughes, As-rigid-as-possible shape manipulation, ACM Trans. Graph. 24 (3) (2005) 1134–1141.

[3] A. Derouet-Jourdan, F. Bertails-Descoubes, J. Thollot, Stable inverse dynamic curves, ACM Trans. Graph. 29 (6) (2010) 137:1–137:10.

[4] G. Romano, M. Diaco, C. Sellitto, Tangent stiffness of elastic continua on manifolds, in: S. Rionero, G. Romano (Eds.), Trends and Applications of Mathematics to Mechanics, Springer Milan, 2005, pp. 155–184.

[5] J. Argyris, H. Balmer, J. Doltsinis, P. Dunne, M. Haase, M. Kleiber, G. Malejannakis, H.-P. Mlejnek, M. Müller, D. Scharpf, Finite element method - the natural approach, Computer Methods in Applied Mechanics and Engineering 17-18, Part 1 (0) (1979) 1 – 106.

[6] R. Barzel, Faking dynamics of ropes and springs, IEEE Comput. Graph. Appl. 17 (1997) 31–39.

[7] T. Hughes, The Finite Element Method: Linear Static and Dynamic Finite Element Analysis, Prentice-Hall, Englewood Cliffs, NJ,, 1987.

[8] F. C. E. Cosserat, Théorie des corps déformables, Hermann et Fils, 1909, (Translation: Theory of deformable bodies, NASA TT F-11 561, 1968).

[9] J. H. Maddocks, Stability of nonlinearly elastic rods, Archive for Rational Mechanics and Analysis 85 (1984) 311–354.

[10] D. K. Pai, Strands: Interactive simulation of thin solids using cosserat models, Computer Graphics Forum 21 (3) (2002) 347–352.

[11] M. Grégoire, E. Schömer, Interactive simulation of one-dimensional flexible parts, Computer-Aided Design 39 (8) (2007) 694 – 707.

[12] J. Spillmann, M. Teschner, Corde: Cosserat rod elements for the dynamic simulation of one-dimensional elastic objects, in: Proceedings of the 2007 ACM SIGGRAPH/Eurographics symposium on Computer animation, SCA '07, 2007, pp. 63–72.

[13] M. Bergou, M. Wardetzky, S. Robinson, B. Audoly, E. Grinspun, Discrete elastic rods, ACM Trans. Graph. 27 (3) (2008) 63:1–63:12.

[14] F. Bertails, B. Audoly, M.-P. Cani, B. Querleux, F. Leroy, J.-L. Lévêque, Super-helices for predicting the dynamics of natural hair, ACM Trans. Graph. 25 (3) (2006) 1180–1187.

[15] M. Botsch, O. Sorkine, On linear variational surface deformation methods, IEEE Transactions on Visualization and Computer Graphics 14 (1) (2008) 213–230.

[16] As-rigid-as-possible curve editing demonstration applet, (accessed on 07.04.2011) url = http://www-ui.is.s.u-tokyo.ac.jp/ takeo/research/rigid/curve/index.html,.

[17] E. Reissner, On one-dimensional large-displacement finite-strain beam theory, Studies in Applied Mathematics 52 (1973) 87–95.

[18] J. Simo, L. Vu-Quoc, A three-dimensional finite-strain rod model. part ii: Computational aspects, Computer Methods in Applied Mechanics and Engineering 58 (1) (1986) 79 – 116.

[19] ABAQUS, Inc., Dassault Systèmes, ABAQUS Analysis Users Manual, version 6.7 ed. Edition (2007).

[20] B. Nour-Omid, C. Rankin, Finite rotation analysis and consistent linearization using projectors, Computer Methods in Applied Mechanics and Engineering 93 (3) (1991) 353 – 384.

[21] M. Müller, J. Dorsey, L. McMillan, R. Jagnow, B. Cutler, Stable real-time deformations, in: Proceedings of the 2002 ACM SIGGRAPH/Eurographics symposium on Computer animation, pp. 49–54.

[22] M. Hauth, W. Strasser, W.: Corotational simulation of deformable solids, in: In: Proc. WSCG, Vol. 12, 2004, pp. 137–145.

[23] J. Georgii, R. Westermann, Corotated finite elements made fast and stable., in: F. Faure, M. Teschner (Eds.), VRIPHYS, Eurographics Association, 2008, pp. 11–19.

[24] A. Kassimali, Structural Analysis, Thomson Inc., 2005.

[25] M.A., Crisfield, A fast incremental/iterative solution procedure that handles snap-through, Computers and Structures 13 (1-3) (1981) 55 – 62.

[26] M. A. Crisfield, Non-Linear Finite Element Analysis of Solids and Structures: Advanced Topics, 1st Edition, John Wiley & Sons, Inc., New York, NY, USA, 1997.